AAS 03-150

CONTOUR PHASING ORBITS: ATTITUDE DETERMINATION & CONTROL CONCEPTS AND FLIGHT RESULTS

Jozef van der Ha*, Gabe Rogers*, Wayne Dellinger*, James Stratton*

The CONTOUR spacecraft was launched on July 3, 2002 and placed in an Earth phasing orbit that lasted about 6 weeks. The spacecraft was kept in a spin-stabilized configuration throughout this period. The main objective during this phase was to achieve the proper orbit and attitude parameters for the injection (by means of a Solid Rocket Motor) into a heliocentric trajectory to Encke's comet. The paper describes the main characteristics of the attitude determination and control concepts behind the design of the CONTOUR spin mode. The Earth Sun Sensor operating concept, attitude determination algorithms, as well as attitude accuracy estimates are addressed. Next, the execution of attitude maneuvers, the maneuver calibration concept, and the design of the propulsion system are discussed. Finally, flight results such as the performances of the attitude maneuvers are presented.

INTRODUCTION

The CONTOUR (Comet Nucleus Tour) mission is part of NASA's Discovery Program and aimed at performing imaging and other science explorations of at least two comet nuclei: Encke and Schwassmann-Wachmann-3. The CONTOUR spacecraft was launched on July 3, 2002 and placed in an Earth phasing orbit with a period of 1.75 days by a Delta-7425. The injection into a heliocentric trajectory on course to Encke's comet took place on August 15. Unfortunately, a mishap occurred near the end of the STAR-30BP Solid Rocket Motor (SRM) firing and contact with the spacecraft could not be re-established[1].

During its 6 weeks of Earth phasing orbits, CONTOUR was kept in a spin-stabilized mode with nominal spin rates of 20 and 60 rpm. A large number of orbit and attitude maneuvers were executed with the objective to achieve the most favorable orbit and attitude parameters as well as hydrazine mass at the time of the SRM burn. The spacecraft performance was practically flawless throughout the phasing orbits. This paper summarizes the pertinent design concept as well as the observed in-flight performances of the guidance and control capabilities that supported the spin mode used throughout the phasing orbits.

ATTITUDE DETERMINATION CONCEPT

Earth-Sun Sensor

The orientation of the spacecraft spin axis in inertial space was determined by means of measurements generated by an integrated Earth-Sun Sensor (ESS) unit manufactured by Galileo Avionica of Florence, Italy. This sensor has been used extensively in geo-stationary transfer orbit operations for over 25 years and has shown excellent reliability. The Sun sensor produces pulses when the Sun crosses over the meridian and skew slits during each spin revolution (Figure 1). The spin rate follows from the time difference between two successive meridian pulses, and the Sun angle θ is calculated from the delay between the meridian and skew slit pulses.

*Applied Physics Laboratory, The Johns Hopkins University, 11100 Johns Hopkins Rd, Laurel, MD 20723-6099, USA; e-mail: JvdHa@aol.com, Gabe.Rogers@jhuapl.edu, Wayne.Dellinger@jhuapl.edu, James.Stratton@jhuapl.edu.

The Earth sensor has two static pencil-beams oriented at angles μ_i (with μ_1 = 60 and μ_2 = 65 degrees) relative to the positive spin axis. The fundamental measurements consist of the Space/Earth (S/E) and Earth/Space (E/S) crossing times of the Earth's Infra-Red horizon. Figure 2 shows that these crossings (in combination with the Sun sensor's meridian slit crossing time) result in measurements of the Sun-Earth Azimuth Angles (SEAA) α_i and the Half-Chord Angles (HCA) κ_i for each of the pencil-beams (i = 1, 2). The SEAA angle α represents the dihedral rotation angle that is formed by the spacecraft spinning (about its Z axis) from the Sun's meridian up to the meridian containing the center of the Earth.

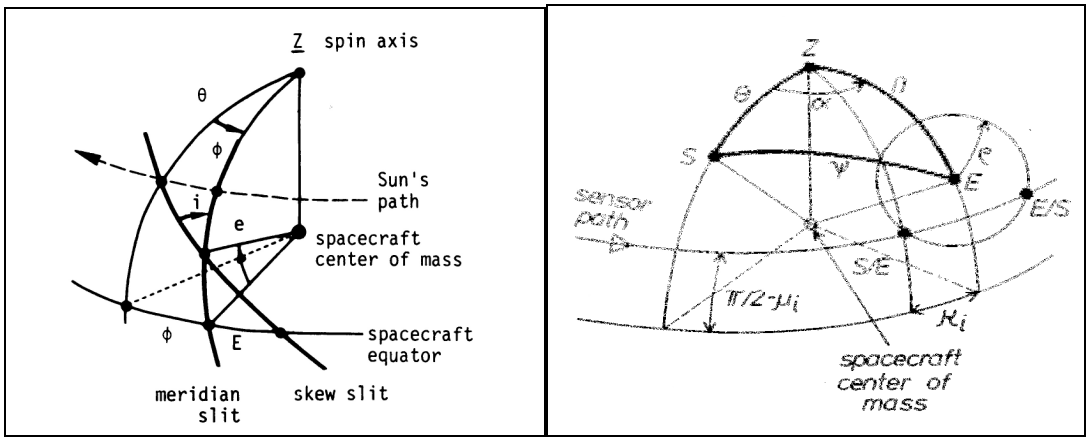

Figures 1 & 2 - Measurement Principles and Geometries for Sun Sensor & Earth Sensor

The design of the Earth sensor has been customized for the CONTOUR-specific phasing orbits with perigee altitudes near 200 km and apogees of about 18 Earth radii (see Ref. 1). It delivers its most accurate performance in the altitude range from about 50000 to 60000 km altitude, which corresponds to the location of the Earth sensor coverage intervals for a spin axis attitude close to the SRM firing direction.

Figure 3 illustrates that the sensor coverage intervals occur in the region after the apogees of the phasing orbits under the selected pencil beam alignment conditions and for the nominal SRM firing attitude direction. The geometrical conditions of the Sun and Earth vectors with a Sun-Earth angle ψ of about 55 degrees in mid August are fairly favorable in terms of expected attitude determination accuracy.

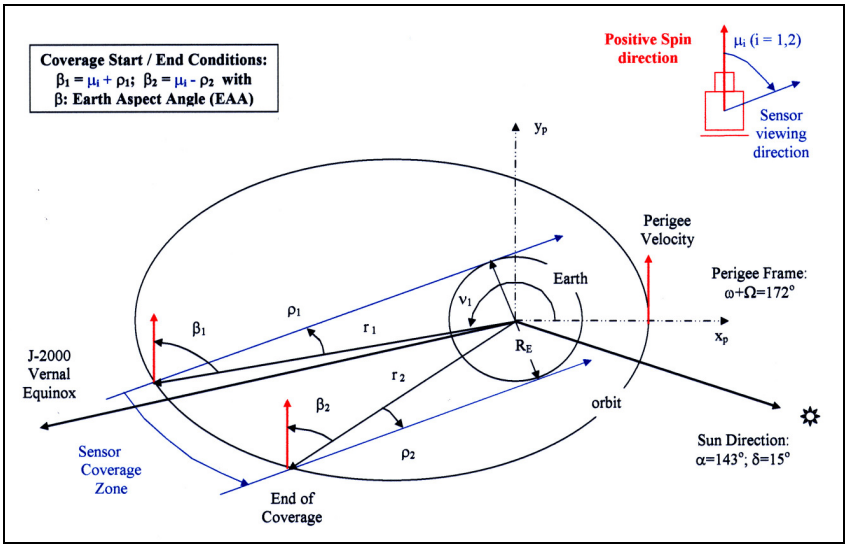

Figure 3 - Earth Sensor Coverage Conditions (Projected View)

Attitude Determination Principles

The most critical requirement for the attitude pointing is imposed by the precision of the thrust direction of the Solid Rocket Motor (SRM): i.e., a half-cone angle of less than 0.75 degrees (including knowledge and control). A pointing error of this magnitude would require a correction of at least 25 m/sec in terms of delta-v that would need to be delivered by the hydrazine thrusters during the heliocentric trajectory.

Figure 4 illustrates the nominal evolution of the measured half-chord angles κ_i (for the two pencil-beams i = 1, 2) as a function of the decreasing Earth Aspect Angle (EAA) β over the coverage intervals. Also shown is the evolution of the apparent Earth radius $\rho(\beta)$ as seen from the spacecraft's position in its orbit.

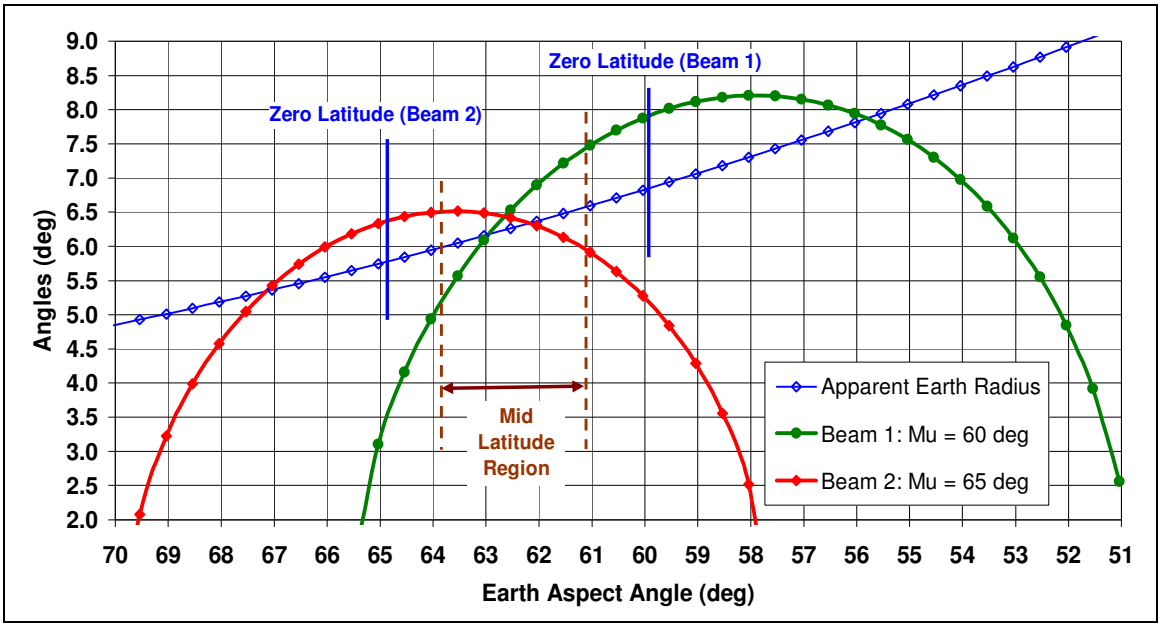

Figure 4 - Half-Chord Angles and Apparent Earth Radius vs. Earth Aspect Angle

The half-chord angles κ_i shown in Figure 4 are derived from the familiar measurement equations for an Earth sensor with nominal pencil-beam mounting alignments of $\mu_1 = 60$ and $\mu_2 = 65$ degrees (Figure 2):

$$\cos\mu_i \cos\beta + \sin\mu_i \sin\beta \cos\kappa_i = \cos\rho \qquad (i = 1, 2) \qquad (1)$$

It should be noted that (during in-flight operations) the chord angles κ_i form the measurements from which the EAA β needs to be determined. The quality and usefulness of the Earth sensor data vary substantially during the few hours of Earth sensor coverage in accordance with the lengths of the scanned chords and the geometrical sensitivity conditions (Ref. 2). The smaller chords are not useful because of the relatively high systematic errors due to the 'near-tangential' Earth crossings. The larger chords, on the other hand, have a favorable crossing geometry but the attitude determination error may be relatively large because of the low measurement sensitivity when scanning in the equatorial region (near the zero latitudes shown in Figure 4): a small error in the measured chord angle results in a large change in the calculated Earth aspect angle.

The best conditions in terms of the resulting attitude determination accuracy occur when the pencil-beams scan the so-called 'mid-latitude' regions of the Earth corresponding to latitude bands between about 10 and 40 as well as -10 and -40 degrees. It may be noted that the 'latitudes' as used here refer to characteristics of the pencil-beam scans and do not necessarily correspond to the familiar geographical Earth latitudes. The combined mid-latitude regions for both pencil-beams under the nominal SRM attitude conditions would correspond to Earth aspect angles in the range from about 61 to 64 degrees as shown in Figure 4.

Two different software programs were employed for attitude determination support during the phasing orbits while CONTOUR was kept in spin-stabilized mode:

1. **Equal-Chord Method (ECM):** this method makes use of a single Earth aspect angle, namely at the time when the chords produced by each of the two pencil-beams are exactly equal; an attitude estimate is obtained by means of a geometrical method involving also the Sun and SEAA angles

2. **Fine Attitude Determination (FAD):** this method uses a batch of Sun and Earth sensor data collected over about an half-hour interval (within the combined mid-latitude region); it produces a precise attitude estimate by means of a 'Weighted Least-Squares' estimation algorithm.

Equal Chord Method

Even though this method is not widely used, it has a number of favorable characteristics (first mentioned in Ref. 3) and a relatively straightforward mathematical formulation. It uses a short interval of Earth sensor measurements around the crossing of the chords produced by the two pencil-beams. The actual crossing time t_e is determined from the quadratic fits of the two arcs of Half-Chord Angle measurements κ_i that are produced by the two pencil beams ($i = 1, 2$): the time t_e provides immediately the reference Earth vector $\underline{\mathbf{E}}_e$.

The Earth Aspect Angle (EAA) β_e at the crossing time t_e can readily be established by subtracting the functional relationships for the two half-chord angles κ_i given in equation (1) and illustrated in Figure 4:

$$\beta_e = \arctan \{\tan\mu / \cos\kappa_e\} \cong \mu + \tfrac{1}{4}\, \kappa_e^2 \sin(2\mu) + O(\kappa_e^4) \qquad (2)$$

Here, μ is the mean value of the two pencil-beam mounting angles relative to the spin axis (i.e., $\mu = 62.5^o$ for CONTOUR's design values) and κ_e is the measured half-chord angle at the time t_e. It can be seen from the simulated results shown in Figure 4 that $\kappa_e \cong 6.4$ degrees. It follows immediately from equation (2) that the Earth aspect angle β_e at the time of equal chords will be $\beta_e \cong 62.6$ degrees with very good accuracy.

Measurement errors in the half-chord-length κ_e do not have an appreciable effect on the resulting β_e since the sensitivity of the EAA β_e to errors in κ_e is small: $|\partial\beta_e/\partial\kappa_e| \cong 0.05$. Furthermore, bias errors in the Earth's Infra-Red horizon have largely been eliminated since the apparent Earth radius does not appear in equation (2) due to the subtraction of the two chords. There may of course be errors that are induced by the non-uniformity of the Earth's Infra-Red radiance profile (since the two pencil-beams are scanning over different parts of the Earth) but these error effects will be fairly small. Therefore, sensor mounting misalignments and/or spacecraft balancing imperfections will most likely be the main contributors to β_e errors.

In addition to the EAA β_e calculated at the time of equal chords, the Equal Chord Method makes use of the Sun Aspect Angle (SAA) ϑ_e and the Sun-Earth Azimuth Angle (SEAA) α_e which is the mean value of the SEAA measurements delivered by the two beams. The complete set of measurement equations is given by:

$$\underline{\mathbf{Z}} \bullet \underline{\mathbf{S}}_e = \cos\vartheta_e; \quad \underline{\mathbf{Z}}_e \bullet \underline{\mathbf{E}}_e = \cos\beta_e; \quad \underline{\mathbf{Z}} \bullet (\underline{\mathbf{S}}_e \times \underline{\mathbf{E}}_e) = \sin\vartheta_e \sin\beta_e \sin\alpha_e \qquad (3)$$

As long as the Sun and Earth vectors are not co-linear, a unique attitude vector $\underline{\mathbf{Z}}$ can be derived from these three equations (note: $\underline{\mathbf{Z}}$ must be normalized because of measurement errors, Ref. 4). In geometrical terms, the first two equations provide two solutions representing the intersections of the two cones with half-cone angles ϑ_e and β_e and centered around the instantaneous Sun and Earth vectors $\underline{\mathbf{S}}_e$ and $\underline{\mathbf{E}}_e$. The measurement α_e provides the resolution of the two-fold ambiguity in the attitude solution through the third equation.

Thus, the ECM attitude determination method does not require any a priori attitude knowledge and is relatively straightforward in terms of implementation effort. Furthermore, the method is extremely 'robust' in terms of sensitivity to chord-length errors and to variations in the apparent Earth radius induced for instance by variations in the Earth's Infra-Red radiance profile.

Fine Attitude Determination

The Fine Attitude Determination (FAD) method uses a batch of Sun and Earth sensor measurements collected over an interval of about 0.5 hr duration while the pencil-beams are scanning over the combined mid-latitude region. The estimation algorithm uses a system of measurement equations similar to equations (3) but expressed in terms of the batch of observation angles ϑ_k, β_k, α_k collected at the instants t_k (k = 1,…, K) with K of the order of 1000 to 2000 at the 60 rpm spin rate. Whereas the motion of the Sun's position in inertial space is practically negligible over a 0.5 hr interval, the changing Earth vector positions $\underline{\mathbf{E}}_k$ must be taken into account. A representative Sun-Earth Azimuth Angle measurement α_k at time t_k is provided by the mean value of the two individual SEAA measurements $\alpha_i(t_k)$ delivered by the two pencil-beams.

The model for the EAA measurements $\beta_k = \beta(t_k)$ is more complicated since there are two solutions $\beta_k^{(+)}$ and $\beta_k^{(-)}$ that satisfy a given half-chord angle measurement, i.e. the scans above and below the 'equatorial' Earth crossing, as can be seen from equation (1) and Figure 2. In order to eliminate this ambiguity an a priori reference attitude $\underline{\mathbf{Z}}_{ref}$ will be introduced. The attitude established by the ECM method is obviously a suitable candidate for $\underline{\mathbf{Z}}_{ref}$. The differences $\delta\kappa_i(t_k)$ between the actual half-chord measurements $\kappa_i(t_k)$ and the predicted (on the basis of the reference attitude) measurements $\kappa_{i,ref}(t_k)$ will be used in the measurement model. After linearization of the two measurement equations in (1), the differences in the Earth Aspect Angles $\delta\beta_i$ can be expressed in terms of $\delta\kappa_i$ at the times t_k for each pencil-beam i = 1, 2:

$$\delta\beta_i(t_k) = f_i(t_k)\, \delta\kappa_i(t_k) \qquad (i = 1,2;\ k = 1, \dots, K) \tag{4}$$

The functions $f_i(t_k)$ represent complicated expressions of the known quantities μ_i, $\kappa_{i,ref}(t_k)$, and $\beta_{ref}(t_k)$. It is important to recognize that the functions $f_i(t_k)$ vary in accordance with the varying sensitivities of the EAA $\beta_i(t)$ as a function of the chord-length angles $\kappa_i(t)$ over the coverage intervals. A single solution $\delta\beta(t)$ may be established by using a linear weighted combination of the individual results for the two pencil-beams:

$$\delta\beta(t_k) = w(t_k)\, f_1(t_k)\, \delta\kappa_1(t_k) + [1\text{-}w(t_k)]\, f_2(t_k)\, \delta\kappa_2(t_k) \tag{5}$$

It makes sense to select the weights $w_k = w(t_k)$ in such a way that the resulting variance of $\beta_k = \beta(t_k)$ will be minimal: the 'optimal' (in a minimum-variance sense) solution $\delta\beta_k^*$ can be established by requiring that $\partial\{\sigma_\beta^2\}/\partial w$ vanishes at every point t_k. It may be noted that the variance $\sigma_\beta^2 = E\{\beta^2\} = E\{(\delta\beta)^2\}$ since the values of the reference Earth aspect angle $\beta_{ref}(t_k)$ are known a priori on the basis of the selected $\underline{\mathbf{Z}}_{ref}$. For convenience, it will be assumed that the chord measurements are uncorrelated and will have equal variances σ_κ^2 for the two pencil-beams throughout the mid-latitude region of the coverage interval.

The solutions for the weights w_k can be shown to be equal to $w = f_2^2/(f_1^2 + f_2^2)$ at every point t_k. It follows that the weights of the 60-degree beam will dominate those of the 65-degree beam during the first part of the coverage interval (i.e., for EAA > 62.35 degrees) and vice versa for the second part. The differences are of the order of 2 to 3 at the start and end of the half-hour data interval centered around the time of equal chords. This result can be shown to be consistent with the nature of the evolution of the sensitivity functions $|\partial\beta/\partial\kappa_i|$ for the two pencil-beams.

Finally, the resulting minimum-variance Earth aspect angle and the associated variance are as follows:

$$\beta^*(t_k) = \beta_{ref}(t_k) + \{\delta\kappa_1(t_k)/f_1(t_k) + \delta\kappa_2(t_k)/f_2(t_k)\}/F(t_k); \qquad \sigma_\beta^2(t_k) = \sigma_\kappa^2/F(t_k) \tag{6}$$

Here, the auxiliary function $F(t_k)$ denotes $1/f_1^2 + 1/f_2^2$ at time t_k. A representative worst-case value for the CONTOUR coverage conditions is given by $F \cong 0.5$ so that $\sigma_\beta^2 \cong 2\sigma_\kappa^2$.

A weighted least-squares solution $\underline{\mathbf{Z}}^*$ for the attitude vector can be established on the basis of the batch of 'observation angles' ϑ_k, β_k^*, and α_k at the times t_k (k = 1, …, K) in the following form (see, for instance, Ref. 4, equations 45-48):

$$\underline{\mathbf{Z}}^* = [P]\,\Sigma_k\,\{\cos\vartheta_k\,\underline{\mathbf{S}}_k/\sigma_S^2 + \cos\beta_k\,\underline{\mathbf{E}}_k/\sigma_E^2 + \sin\vartheta_k\,\sin\beta_k\,\sin\alpha_k\,(\underline{\mathbf{S}}_k \times \underline{\mathbf{E}}_k)/\sigma_N^2\} \qquad (7)$$

Here, [P] denotes the covariance matrix of the attitude vector $\underline{\mathbf{Z}}^*$ and σ_S^2, σ_E^2, σ_N^2 represent the variances of the observations (note that these variances have been assumed to remain constant over the data interval):

$$\sigma_S^2 = \sigma_\theta^2\,\sin^2\theta; \quad \sigma_E^2 = \sigma_\beta^2\,\sin^2\beta; \quad \sigma_N^2 = \sigma_N^2(\theta, \beta, \alpha, \sigma_\theta^2, \sigma_\beta^2, \sigma_\alpha^2) \qquad (8)$$

After selecting a reference frame for the attitude vector, it will be possible to establish explicit expressions for the state covariance matrix [P] in terms of the results of the three variances given in (8).

Attitude Determination Accuracy

It is important to distinguish between random and systematic errors in the attitude determination process: typical random errors in the amplitudes of the ESS measurements are less than 0.001 degree for the Sun aspect angle and about 0.02 degrees for the Half-Chord and Sun-Earth Azimuth Angles measured by the Earth sensor. It is obvious that random errors have no appreciable effect on the accuracy of the attitude estimate, in particular when using a batch of hundreds or more individual measurements. Systematic errors (also known as 'biases'), on the other hand, usually have significant impacts on the achievable attitude accuracy. Furthermore, their adverse effects can not be attenuated by using more measurements.

Systematic errors may be induced for instance by any of the following sources:

- Local variations in the Earth's Infra-Red horizon: 0.3 degrees (North-South, worst-case)
- Spacecraft dynamic imbalance (including fuel imbalance): 0.1 degrees (worst-case)
- Residual sensor calibration errors: 0.05 degrees (worst-case)
- ESS mounting and spacecraft alignment errors: 0.03 degrees (worst-case)
- Earth and Sun ephemeris errors: 0.02 degrees (worst-case)
- Thermal effects (structural distortions and electronic effects): 0.02 degrees (worst-case)

Of particular interest are the effects induced by spacecraft balancing errors. The in-flight 'dynamical' spin axis (which corresponds to the actual maximum principal inertia axis) will be 'tilted' with respect to the designated 'geometrical' spin axis (which has been the reference for the mounting of the ESS unit). There are two main contributors to the dynamic imbalance:

1. Measurement threshold of the equipment used for the pre-Launch balancing operations: this may result in a worst-case spin axis tilt of the order of 0.04 degrees;
2. Imbalance induced by the asymmetric use of fuel in the two tanks: this imbalance can be kept well below 1 kg by an appropriate strategy for switching between the two tanks in-between maneuvers: the 1 kg fuel imbalance would correspond to a tilt angle of about 0.08 degrees.

Realistic predictions for the effects of the systematic errors on the actual numerical values of the angles used in the measurement model can not easily be established but conservative limits may be the following:

$$\Delta\theta < 0.1^o; \;\; \Delta\kappa < 0.2^o; \;\; \Delta\alpha < 0.3^o; \;\; \Delta\mu < 0.1^o; \;\; \Delta\rho \text{ and } \Delta\psi < 0.02^o \qquad (9)$$

The effect of a particular systematic error on the resulting attitude accuracy may be evaluated by means of a covariance analysis for the single-frame attitude solution based on these input biases (e.g., Ref. 2). A representative explicit formula for the resulting 'attitude error' (i.e., the angular deviation of the unit-vector along the spin axis) may be represented by the trace of the covariance matrix [P] introduced in equation (7):

$$\sigma_{attitude} \cong \{\sigma_S^2 + \sigma_E^2 + \sigma_N^2\}^{1/2}/\sin\psi \qquad (10)$$

After substitution of the relevant input parameters, an expected worst-case attitude error of the order of 0.5 degree follows for the CONTOUR-specific conditions prior to the firing of its SRM in mid August 2002.

ATTITUDE CONTROL CONCEPT

Attitude slew maneuvers were performed by a set of 4 hydrazine thrusters (see Figure 10 below) firing in pulsed mode to deliver a precession torque that changes the direction of the angular momentum vector (and thus also the orientation of the spacecraft spin axis) in inertial space. The selected thrusters form a 'balanced' set, which implies that the resulting perturbing effects on the orbit will be negligible. Also the capability for spin control maneuvers was provided and was actually used in-flight to perform the spin-down from 60 to 20 rpm shortly after Launch and the spin-up back to 60 rpm prior to the SRM firing.

When executing attitude maneuvers it is possible to control the direction of the spin axis motion by selecting the appropriate timing of the thrust pulse initiation within each spin revolution. This can be achieved by introducing a constant delay time for these initiations with respect to the occurrence of the Sun sensor meridian pulse. The required delay time is calculated on-ground beforehand and up-linked to the spacecraft along with the number of thrust pulses and the firing duration of the pulses. The resulting motion of the spin axis on the celestial sphere (under a constant delay angle) follows a so-called rhumb path as shown in Figure 5. More details on rhumb-line maneuvers are provided in Wertz [5] (pp. 651-654).

In order that the deviation of the attitude pointing direction during a long attitude slew maneuver can be kept within acceptable bounds, it is necessary to perform careful calibrations of the effective thrust level, the rhumb angle (or heading direction) as well as spin rate. An elaborate maneuver calibration scheme was implemented as part of the first 180-degree slew (i.e., the so-called 'Flip' maneuver) that was required for establishing the proper attitude for executing an orbit maneuver at the time of the second perigee (Ref. 1).

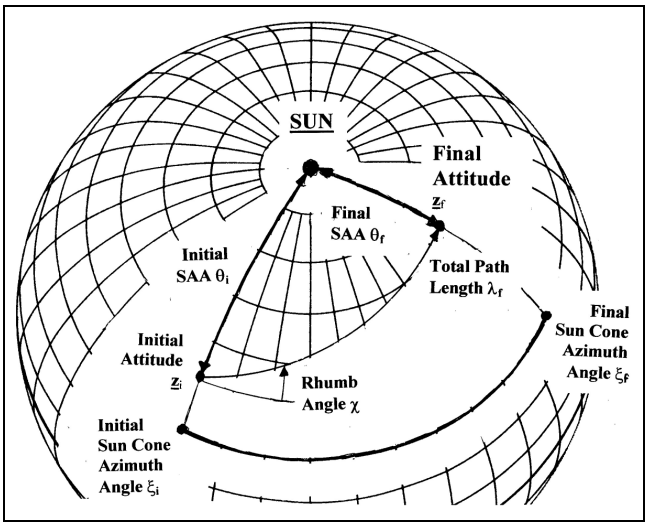

Figure 5 – Geometry of a Rhumb-Line Attitude Maneuver

Figure 6 illustrates the Flip maneuver strategy. The first leg of the Flip maneuver is about 19 degrees long and has a rhumb angle of (nominally) 90 degrees so that the attitude vector will move along a meridian circle in the direction towards the Sun. This results in a 'pure' Sun angle variation so that a very precise calibration of the maneuver path-length λ_f can be established on the basis of the measured change in Sun aspect angle over this maneuver leg. This is equivalent to the calibration of the effective thrust level performance factor P_{thrust} (to a precision of the order of 0.5 %):

$$P_{thrust} = \lambda_{f,\,measured} / \lambda_{f,\,prepared} \cong \Delta\theta_{measured} / \Delta\theta_{prepared} \tag{11}$$

The second leg of the Flip maneuver is about 57 degrees long and follows a direction that is perpendicular to the first leg. The (nominal) rhumb angle that will be maintained throughout this leg is 180 degrees so the attitude will move along the Sun cone, which means that the Sun aspect angle should remain constant

during this maneuver leg. Therefore, any observed change in Sun aspect angle over the maneuver leg must be caused by an error in the effective rhumb angle χ. This is equivalent to the calibration of the effective mean centroid delay angle of the thrust pulses of the selected set of thrusters (to a precision of about 0.1^o):

$$\Delta\chi = \chi_{measured} - \chi_{prepared} \cong \Delta\theta_{measured} / \lambda_{f,\ prepared} \tag{12}$$

It has been assumed here that the thrust level calibration result in (11) has already been incorporated in the prepared path length $\lambda_{f,\ prepared}$ (otherwise, a more intricate formula should be used).

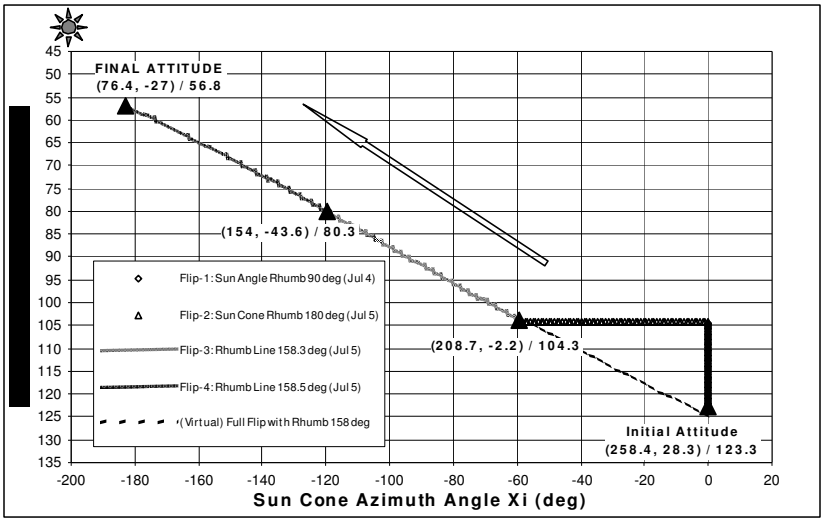

Figure 6 – Design of 180-degree Flip Maneuver, Including Calibration Strategy

The nominal length of the second leg was selected so that its end-point lies precisely on the great circle of the full 180-degree Flip maneuver. Furthermore, the Flip maneuver strategy included a useful independent confirmation of the achieved attitude pointing at this time with the aid of an Earth sensor coverage interval that occurred shortly after conclusion of the second leg. By employing the calibration results as well as the observed spin variations established over the first two maneuver legs, it was possible to reduce the expected error in the final attitude pointing after the remaining two legs (each about 64 degrees long) to less than 3 degrees. The established calibration knowledge was employed for the benefit of all attitude maneuvers throughout the phasing orbits (this implies of course that the same set of thrusters needed to be used).

SOFTWARE DESIGN & IMPLEMENTATION

The software used for ground based attitude determination and control was generated using The Mathworks® Matlab program. The Equal Chord Method and Fine Determination Method algorithms, as well as the algorithms developed to calculate the thruster commands for the maneuvers, were implemented in m-files that were placed under configuration control on a PC in the CONTOUR mission operations center. These m-files would read an input ASCII input file that contained data on the current state of the spacecraft, calibration coefficients, alignment parameters, and desired states following a maneuver.

To determine the attitude of the spin axis, telemetry from the spacecraft was processed and loaded into a Matlab workspace, where the m-files processed it to determine an attitude. The results of each run were recorded in an attitude history file that was used by mission operations as well as by the navigation team. Maneuvers were generated using the current and desired states of the spacecraft. The end result of this process was a maneuver file containing all information needed to change the rate or orientation of the spin axis, or the orbit of the spacecraft. The resulting maneuver files were then transferred to the mission operations team for testing and upload to the spacecraft.

SPIN MODE HARDWARE DESIGN

The hardware implementation for the CONTOUR spin mode was relatively straightforward. The Earth Sun Sensor (ESS) was the source of information for all attitude measurements during this mode as explained above. Figure 7 shows a photograph of the ESS sensor unit taken during spacecraft integration. The unit consists of two Earth sensor pencil-beams and a V-slit Sun sensor. The 'meridian' Sun sensor slit is aligned with the spin axis of the spacecraft and is used to determine the spin rate. This slit serves also as reference for the Earth sensor measurements, which allows the calculation of the Sun-Earth Azimuth Angle (as shown in Figure 2). The 'skew' Sun sensor slit, corresponding to the canted slit in Figure 7, is used along with the meridian slit to determine the Sun angle.

The V-slit Sun sensor is equipped with eight silicon photo-detectors (which are redundant within the principal range of Sun angles from about 60 to 120 degrees) operating in the visible band of the spectrum (from 0.3 to 1.1 μm). Each pencil-beam of the Earth sensor has an immersed thermistor bolometer Infra-Red detector operating in the CO_2 spectral band between 14 and 16.25 μm. The crossing times of the Earth's Infra-Red horizon are obtained through (on-board) processing of the detector measurements.

Output of the ESS sensor consists of six pulses on separate wires corresponding to: the Sun crossing the meridian slit, the Sun crossing the skew slit, space-to-Earth crossing detected by the upper Earth sensor pencil-beam, Earth-to-space crossing detected by the upper Earth sensor, and similar detections by the lower Earth sensor beam.

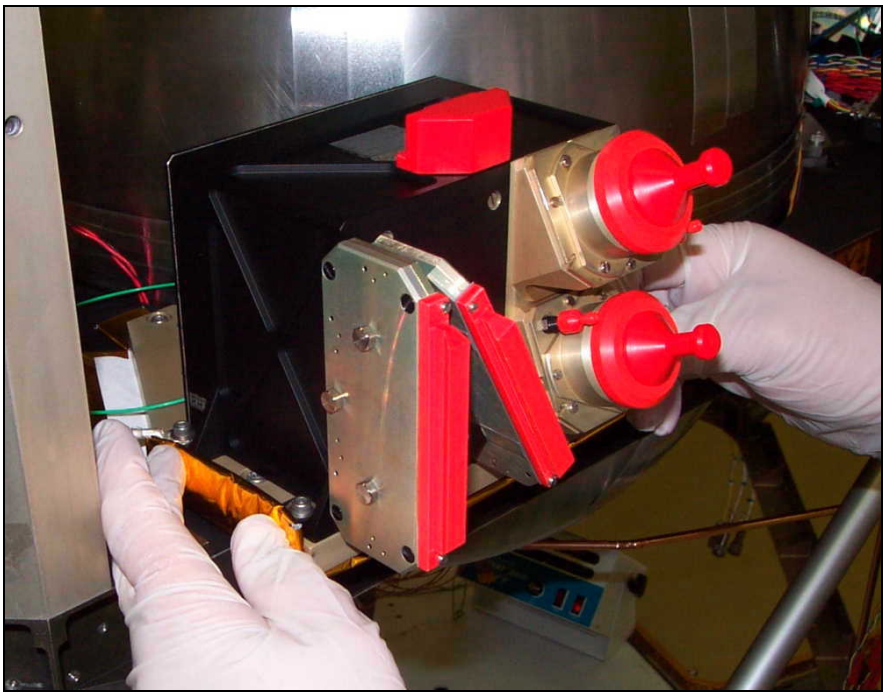

Figure 7 – Earth Sun Sensor Unit during Spacecraft Integration

Figure 8 shows a block diagram of the hardware configuration used for spin mode. The ESS pulses are detected by the Thruster / Attitude Control Card (TAC). Upon detection of the meridian pulse, the TAC counts the number of one-microsecond tics that occur from the time the meridian pulse is detected to the time each of the other five pulses are detected. This timing information is packed for distribution onto the '1553 bus' for receipt by the Command and Data Handling (C&DH) processor and for subsequent transmission to the ground. The timing data are de-commutated by the ground system and then processed by the various attitude estimation algorithms.

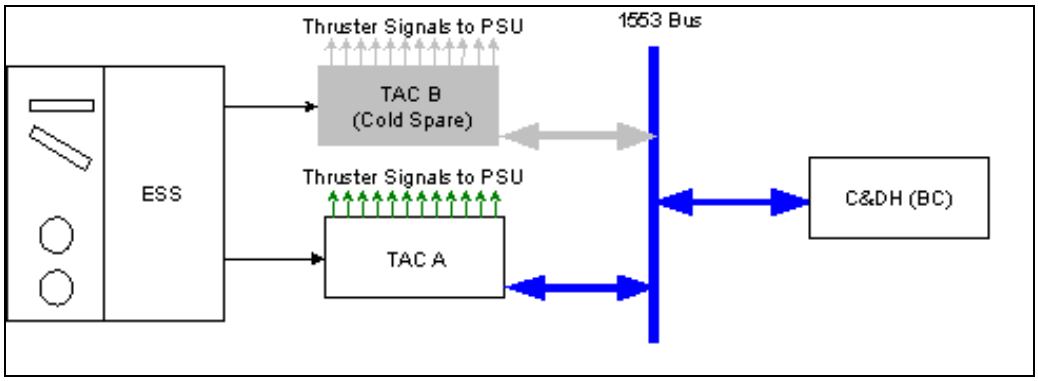

Figure 8 – Block Diagram of Spin Mode Hardware Configuration

Thruster control is equally straightforward. The required thruster firing parameters (consisting of delay time, on-time, number of pulses, etc.) are calculated on-ground and up-linked to the TAC via the C&DH. The TAC then commands the individual thrusters based on the parameter values. The time resolution for commanded thruster firings is one millisecond and the minimum firing duration is 0.125 sec.

PROPULSION SYSTEM DESIGN

A schematic of the CONTOUR Liquid Propulsion System (LPS) is shown in Figure 9. The CONTOUR LPS includes a total of sixteen thrusters: fourteen small 0.2 lb_f thrusters, and two large 5 lb_f thrusters. Orbit delta-v maneuvers (see Ref. 1) are normally performed by means of the two 5-lbs thrusters firing in continuous mode. Orbit correction maneuvers in a radial direction may be delivered by a set of 4 or more radial 0.2 lbs thrusters firing in pulsed mode with prescribed delay angles relative to the Sun meridian pulse (in a similar manner as described above for the attitude reorientation maneuvers).

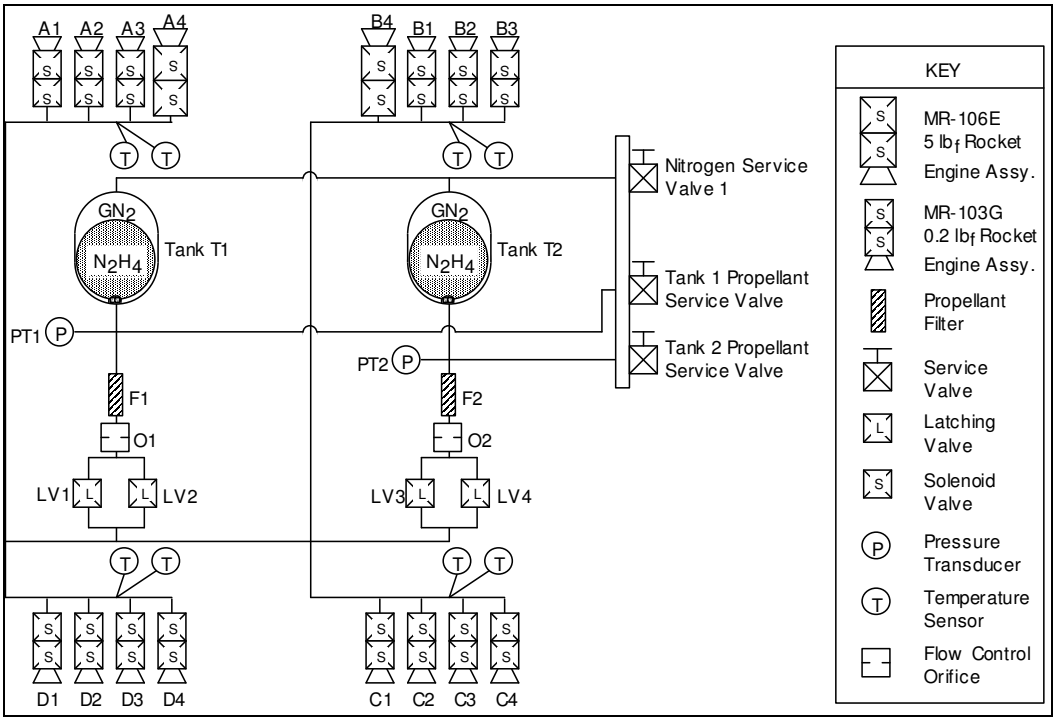

Figure 9 - CONTOUR Liquid Propulsion System Schematic

The thrusters use high purity hydrazine (N_2H_4) and are fed propellant from two propellant/pressurant tanks by simple blow-down. Each thruster contains a series-redundant solenoid valve, redundant valve heaters and redundant catalyst bed heaters. These thrusters are mounted in four different Rocket Engine Modules (REM's), which are positioned as shown in Figure 10. The design provides 'near-pure' couple torques about all three axes as well as both positive and negative ΔV corrections in all three directions. The adjective 'near-pure' refers to the resulting undesirable effects on the orbit: these are typically not more than a few mm/sec after a 180-degree attitude maneuver.

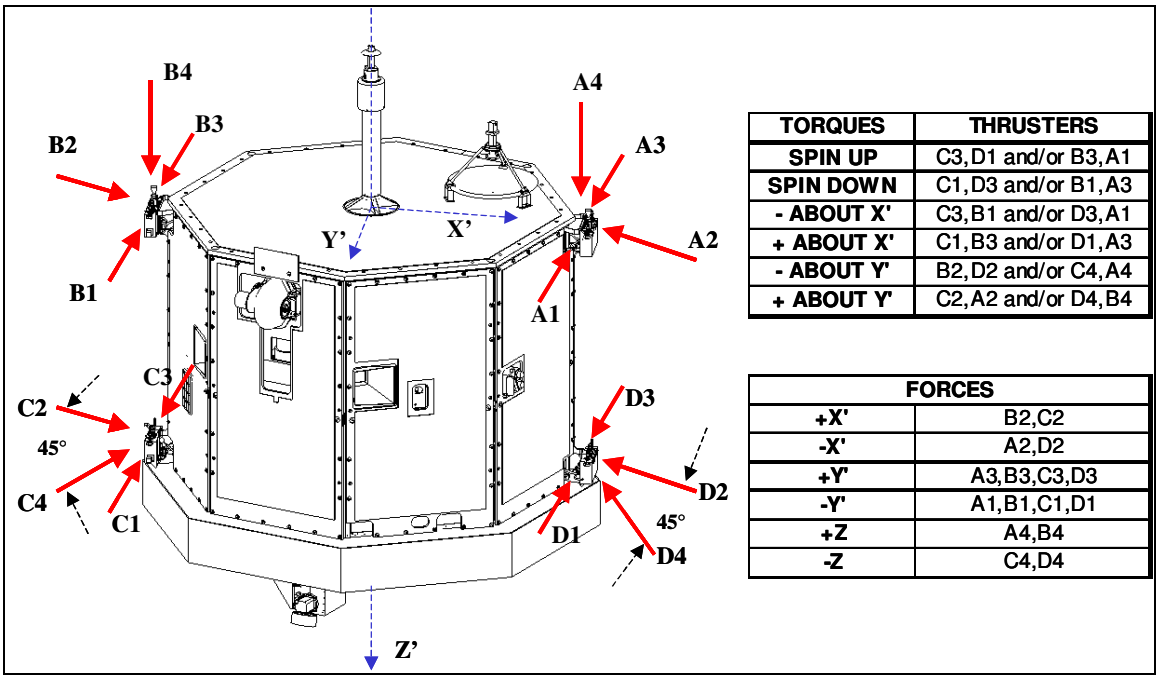

TORQUES	THRUSTERS
SPIN UP	C3,D1 and/or B3,A1
SPIN DOWN	C1,D3 and/or B1,A3
- ABOUT X'	C3,B1 and/or D3,A1
+ ABOUT X'	C1,B3 and/or D1,A3
- ABOUT Y'	B2,D2 and/or C4,A4
+ ABOUT Y'	C2,A2 and/or D4,B4

FORCES	
+X'	B2,C2
-X'	A2,D2
+Y'	A3,B3,C3,D3
-Y'	A1,B1,C1,D1
+Z	A4,B4
-Z	C4,D4

Figure 10 – Overview of CONTOUR Thruster Utilization

The LPS tanks are internally pressurized using Nitrogen, and have their ullages manifolded together to minimize the risk of propellant migration due to thermal and pressure variations in the tanks. The ullages of both tanks are pressurized through a single pressurant service valve. Each tank has its own individual pressure transducer, service valve, flow-control orifice, propellant filter, and a parallel redundant set of two latch valves downstream of the filter. Propellant flow paths have been designed such that both tanks are capable of providing propellant for all sixteen thrusters, and switching between propellant tanks (for maintaining the fuel imbalance below the required 1 kg) is possible by using the latch valves. The propellant flow path layout and the selective matching of components result in a nearly identical pressure drop from each tank to the thrusters. Latch valves were also required to meet the Range Safety requirement that there are at least three valve seats between the propellant in the tanks and the outlets of the thrusters.

SUMMARY OF IN-FLIGHT PERFORMANCES

Initial Nutation Damping Performance

The passive nutation damping induced by the energy dissipation effects of the hydrazine fuel was much better than expected. It had been predicted before launch that the Nutation Time Constant (NTC) of the spacecraft would be of the order of 15000 seconds. However, following separation and power up of the ESS the NTC was measured at 500 seconds for a spin rate of 49.5 RPM. At 20 RPM this number rose to 1500 seconds, and at 60 RPM the number dropped to around 300 seconds. Figure 11 shows the nutation damping performance of the spacecraft immediately after separation from the Delta Launcher's third stage.

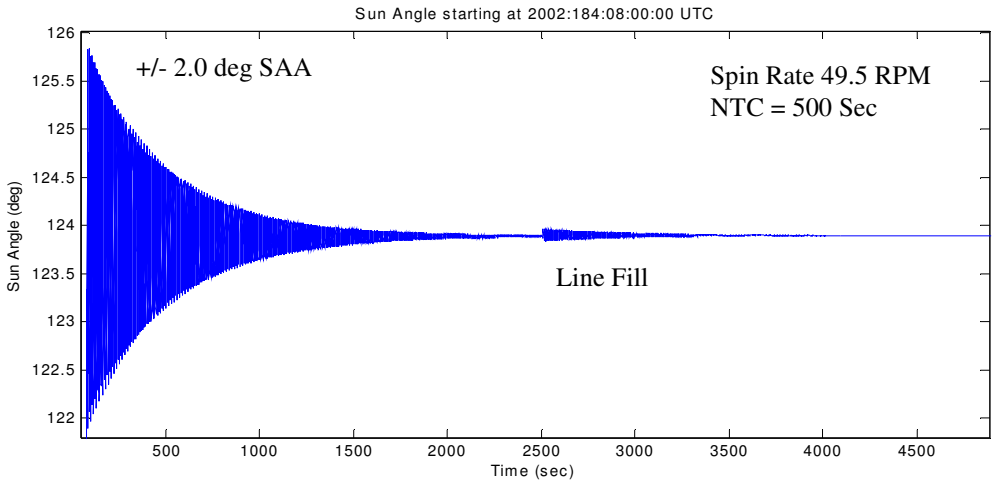

Figure 11 - ESS Measured Sun Angle Following Separation from Delta third Stage at 49.5 rpm.
(Note: the small increase at 2500 seconds was caused by the initial priming of the fuel lines)

Summary of Attitude Maneuvers

During the six weeks of phasing orbits, a total of 12 attitude maneuvers, 7 orbit and 4 spin correction maneuvers were performed. The total length of all slews combined was over 500 degrees and the longest attitude maneuver performed was about 95 degrees. Precise calibrations of thrust-level as well as rhumb angle (including spin effects) were instrumental in achieving adequate pointing precision prior to the execution of the orbit delta-v maneuvers.

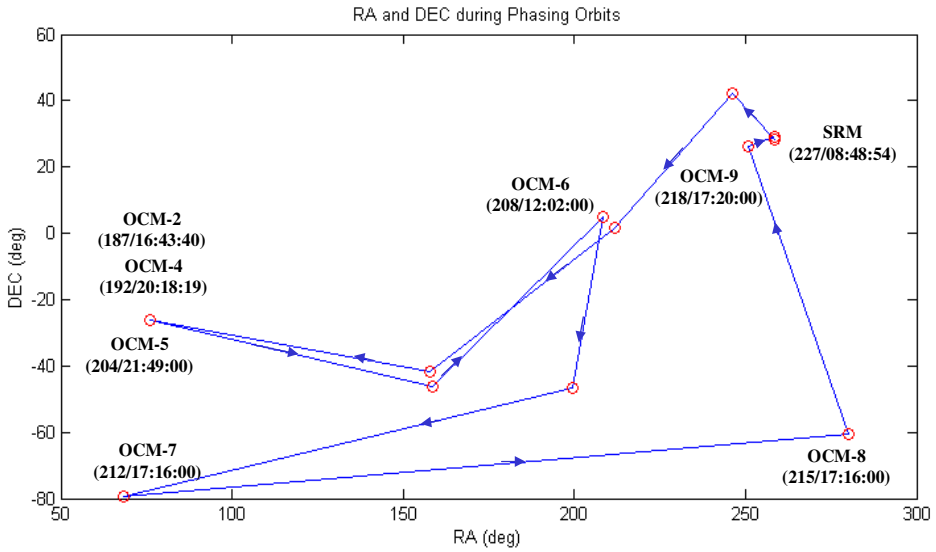

Figure 12 - Right Ascension and Declination of Spin Axis during Phasing Maneuvers

Figure 12 shows the progress of the right ascension (RA) and declination (DEC) of the spin axis during the phasing orbits (it may be noted that the RA and DEC angles are defined with respect to the Earth's equatorial plane within the inertial J2000 reference frame). The objective of each of the attitude maneuvers was to orient the spacecraft in preparation for an Orbit Correction Maneuver (OCM). The separation attitude was very close to the SRM attitude, which is why the spin axis motion appears to create a loop.

Table 1 - Simulated and Observed Data from Attitude Control Maneuvers

ACM	Starting RA/DEC (deg)	End RA/Dec (deg)		Delta (%)	End Sun Angle (deg)		Delta (deg)	Tank Used	Com-ments
		Observed	Simulated		Observed	Simulated			
1	258.40 / 28.30	No ESS Data	246.24 / 42.18	Unknown	106.18	104.3	-(1.83)	1	(1), (2)
2	No ESS Data	211.76 / 1.87	211.80 / 1.65	0.29	105.36	106.13	-(0.77)	1	(1)
3	211.76 / 1.87	No ESS Data	157.70 / -41.86	Unknown	80.29	80.46	0.17	1	(2)
4	No ESS Data	76.2 / -26.22	77.50 / -27.90	1.54	56.6	56.74	0.14	1	(3)
5	76.06 / -26.08	No ESS Data	158.50 / -46.32	Unknown	73.56	73.3	0.26	1	(2)
6	No ESS Data	208.48 / 4.80	208.81 / 4.89	0.25	83.01	82.88	0.13	1	None
7	208.25 / 5.05	No ESS Data	199.52 / -46.70	Unknown	90.78	90.78	0	1	(2)
8	No ESS Data	No ESS Data	68.28 / -79.25	Unknown	103.21	103.12	-(0.09)	1	(2)
9	No ESS Data	No ESS Data	280.32 / -60.38	Unknown	131.8	131.89	0.09	2	(2)
10	No ESS Data	250.65 / 26.39	251.3 / 26.10	0.27	103.87	103.74	0.13	1	(4)
11	250.71 / 25.07	258.56 / 29.10	258.69 / 29.39	3.81	105.69	105.93	-(0.24)	2	(5)
12	258.56 / 29.10	258.66 / 29.21	258.72 / 29.28	36.42	103.73	103.66	-(0.07)	2	(5)

Notes: (1) Simulation deltas are based on distance traveled between ESS measurements.

(2) Simulation accounted for linear spin rate changes during burn.

(3) End RA/DEC based on ESS data post maneuver.

(4) Observed sun angle calibrated for ESS misalignment.

Comments: (1) Calibration Maneuver 10.9% underperformance from model. 37 msec thrust pulse centroid delay.

(2) No ESS data following this maneuver before start of next ACM.

(3) OCM between end of ACM and ESS measurement, which could shift spin axis by +/- 0.2 deg.

(4) SCM between end of ACM and ESS measurement.

(5) Small maneuver. Attitude knowledge uncertainty is large portion of delta uncertainty.

Table 1 provides an overview of the performances of the attitude control maneuvers. It can be seen that after the completion of the two calibration maneuvers (ACM-1 and 2), the difference between the simulated and observed Sun angle was never greater than 0.26 degrees. Most of the difference was due to unanticipated changes in the spin rate. Following a maneuver these changes were substituted into the simulation and the result was a solution that very closely matched truth. Note that the larger percentage deltas for ACM-11 and -12 were due to the fact that the maneuver lengths were relatively small (i.e., only 8 and 0.3 degrees respectively) so that attitude uncertainties have a large effect on the apparent performances.

Thruster Performances & Calibrations

Following each maneuver, and in preparation for each future maneuver, the thrusters were calibrated using observed maneuver performances. Thruster performance was measured against blow-down predictions based on thruster acceptance test calibration data and measurements of the current propellant tank pressure. The thruster performance curves generated during thruster acceptance testing were used throughout the mission to predict thruster performance. Performance variations were modeled as changes in the thruster feed (inlet) pressure. This feed pressure was modeled relative to the measured tank pressure, so that estimates of future feed pressure could be made. This technique provided very accurate and consistent estimates of thruster performances throughout the phasing orbits as shown in Table 1.

Attitude Determination Results

In order to be able to achieve the required attitude determination accuracy use was made of the on-ground 'calibration data' that were measured by the manufacturer prior to delivery of the ESS unit. These data model the delays between the actual ESS pulses and the expected geometric crossing times. In particular, the calibrations of the Earth sensor S/E and E/S crossings are critical since they lead to corrections of the measured chord centers (i.e., SEAA angle) of as much as 1.51^o and 1.31^o for the two beams. Furthermore, the best available knowledge of the ESS mounting angles as measured during spacecraft alignment tests needed to be incorporated. This resulted in a change of almost 14 arc-min in the Sun sensor elevation angle (i.e., $\Delta e = -0.226^o$ with nominal design value $e = 0$) as well as in the pencil-beam mounting angles $\Delta\mu_1 = \Delta\mu_2 = +0.226^o$ relative to their nominal design values of 60 and 65 degrees (see Figures 1 to 3).

Table 2 – Final Attitude Determination Residuals (in Degrees) Prior to SRM Firing on August 15

	Attitude Pointing		Residuals over 0.5 hour near Equal Chords						Distance to SRM Attitude	Attitude Consistency
Solution	RA & DEC		SAA	EAA	HCA-1 & 2		SEAA-1 & 2			
ThBe	258.62	29.27	0.005	0.008	0.23	0.22	0.03	0.22	0.09	0.125
ThBeAl	258.60	29.18	0.023	0.008	0.22	0.21	0.03	0.16	0.16	0.036
RES	258.53	29.10	0.003	0.007	0.20	0.19	0.09	0.10	**0.26**	0.086
ECM	258.64	29.13	0.078	0.008	0.22	0.21	0.07	0.12	0.18	0.093
FAD	258.61	29.15	0.046	0.008	0.22	0.21	0.06	0.13	0.17	Reference
	Averages:		**0.031**	**0.008**	**0.22**	**0.20**	**0.06**	**0.14**	**0.17**	**0.085**

The attitude determination results obtained by the software algorithms were validated by means of a scrutiny of the residuals in the Sun and Earth sensor measurement angles ϑ, κ_1, κ_2, α_1, α_2. These residuals represent the differences between the 'predicted' measurement angles (resulting from simulations based on the applicable attitude estimate) and the actual down-linked sensor measurements over the relevant interval.

Table 2 summarizes the results for the residuals (i.e., their average values over the half hour of sensor data centered on the time of equal chords) during the final coverage interval before the SRM firing. A total of five different attitude determination results are shown in Table 2: the 'spread' or consistency between these attitude solutions provides an indication of the likely remaining error. The best possible estimate is most likely delivered by the Fine Attitude Determination (FAD) solution since it is based on the largest set of measurements. The following list describes the five solutions in increasing order of 'sophistication':

1. **ThBe**: represents the geometric attitude solution based only on the SAA θ_e and the EAA β_e measured at the time of equal chords
2. **ThBeAl**: represents the geometric solution obtained from all three angular observations, namely the SAA θ_e, the EAA β_e and the SEAA α_e all taken at the time of equal chords; the deviation of this attitude result from **ThBe** under point 1 provides an indication of the consistency of the SEAA measurement which is likely the 'weakest' entry due to its sensitivity to the North-South IR effects.
3. **RES**: is the solution that aims at reconciling the observed residuals as well as possible; it is obtained from ThBeAl in an iterative manner by (visually) minimizing the evolution of the differences between the simulated and measured SEAA's over the interval of interest
4. **ECM**: is the result of the ECM software (described in detail above): the main difference with the **ThBeAl** approach lies in the quadratic fitting of the chords over the interval around the equal chords
5. **FAD**: is the result of the FAD software (described in detail above): this is expected to be the most accurate result available as it is based on all available measurements with their applicable weightings over the half hour data interval.

Figure 13 illustrates the locations of these attitude solutions relative to each other as well as the designated SRM attitude in a (linearized) Right Ascension (RA) versus Declination (DEC) diagram. It is seen from Figure 13 and Table 2 that all 5 solutions are contained within a circle of diameter of less than 0.2 degrees, which is indicative of the excellent consistency between all possible solutions. Furthermore, all of the solutions (except for RES) are expected to be within 0.2 degrees from the target SRM attitude as shown in Table 2 above.

Because of the mishap that occurred near the end of the SRM firing, it has unfortunately not been possible to reconstruct the actual attitude error on the basis of the observed delta-v direction delivered during the SRM firing to a very good precision. The available knowledge of the orbits of the three pieces that have been observed would indicate that the error in the attitude orientation during the SRM burn has in any case been below 0.44 degrees. This result represents the maximum of the three reconstructed attitude errors resulting from the analyses of the post-SRM orbits as outlined in Refs. 1 and 7.

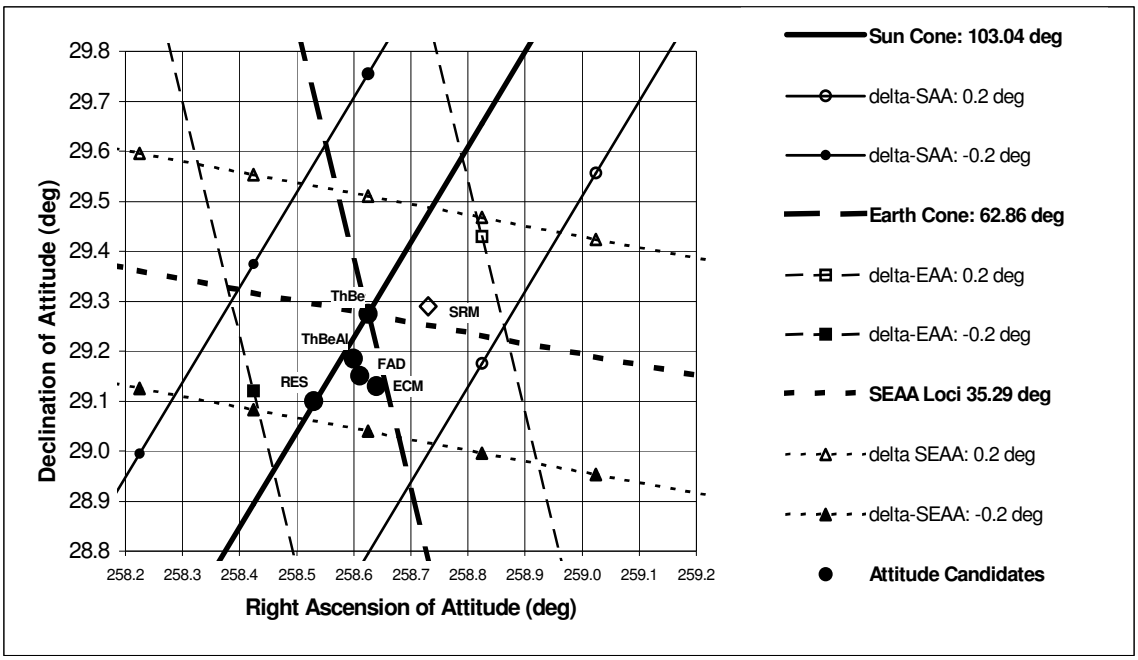

Figure 13 – Attitude Solutions Relative to SAA, EAA & SEAA Loci (August 15)

CONCLUSION

The paper has outlined the concepts underlying the design of CONTOUR's spinning mode that was used throughout the 6 weeks phasing orbits preceding its ill-fated SRM firing. The in-flight results confirm that the minimal and relatively straightforward hardware and software capabilities that have been implemented were able to support all operational requirements with excellent reliability and accuracy performances.

REFERENCES

1. D. W. Dunham et al., "Design and Implementation of CONTOUR's Phasing Orbits", *AAS/AIAA Space Flight Mechanics Meeting*, Ponce, Puerto Rico, February 9-13, 2003, Paper AAS 03-208.

2. J. C. van der Ha, "Attitude Determination Covariance Analysis for Geo-stationary Transfer Orbits", Journal of Guidance, Control, and Dynamics, Volume 9, Number 2, March-April 1986, pp. 156-163.

3. A. S. Fagg, & L. van Holtz , "Application of Simplified Spin Axis Attitude Determination Techniques to ESA Telecom Satellites, *Proceedings of the CNES Symposium on 'Space Dynamics for Geostationary Satellites'*, Cepadues Editions, Toulouse, France, October 1985, pp. 219-226.

4. M. D. Shuster, "Efficient Algorithms for Spin-Axis Attitude Estimation", *The Journal of the Astronautical Sciences*, Vol. XXXI, April-June 1983, pp. 237-249.

5. J. R. Wertz (Editor), *Spacecraft Attitude Determination and Control*, Kluwer, 1978, Section 19.3.

6. Stratton, J., Engelbracht, C., Deboer, J., and J. Morris, "Description of the Liquid Propulsion System of the Comet Nucleus Tour Spacecraft", Paper AIAA-2001-3391.

7. E. Carranza et al., "Navigating CONTOUR using the Noncoherent Transceiver Technique", AAS 03-204, *AAS/AIAA Space Flight Mechanics Conference*, Ponce, Puerto Rico, February 9-12, 2003.